NeuroImage xxx (2010) xxx–xxx

Contents lists available at ScienceDirect

NeuroImage

journal homepage: www.elsevier.com/locate/ynimg

Structural asymmetries of perisylvian regions in the preterm newborn

J. Dubois [a,b,*], M. Benders [a,c], F. Lazeyras [d], C. Borradori-Tolsa [a], R. Ha-Vinh Leuchter [a], J.F. Mangin [e], P.S. Hüppi [a,f]

[a] Geneva University Hospitals, Department of Pediatrics, Geneva, Switzerland
[b] INSERM, U663 (Pediatric Epilepsies and Brain Plasticity), Paris, France; University Paris Descartes, Paris, France
[c] Wilhemina Children's Hospital, Department of Neonatology, Utrecht, Netherlands
[d] Geneva University Hospitals, Department of Radiology-CIBM, Geneva, Switzerland
[e] CEA, LNAO (Computer-assisted Neuroimaging Laboratory), CEA/SAC/DSV/I2BM/ NeuroSpin, Saclay, France
[f] Children's Hospital, Department of Neurology, Harvard Medical School, Boston, MA, USA

ARTICLE INFO

Article history:
Received 7 October 2009
Revised 16 March 2010
Accepted 19 March 2010
Available online xxxx

Keywords:
Cortex
Development
Sulcation
Surface
Premature brain
MRI
Asymmetries

ABSTRACT

During the last trimester of human pregnancy, the cerebral cortex of foetuses becomes greatly and quickly gyrified, and *post-mortem* studies have demonstrated that hemispheres are already asymmetric at the level of Heschl gyrus, planum temporale and superior temporal sulcus (STS). Recently, magnetic resonance imaging (MRI) and dedicated post-processing tools enabled the quantitative study of brain development non-invasively in the preterm newborn. However, previous investigations were conducted either over the whole brain or in specific sulci. These approaches may consequently fail to highlight most cerebral sites, where anatomical landmarks are hard to delineate among individuals. In this cross-sectional study, we aimed to blindly and automatically map early asymmetries over the immature cortex. Voxel-based analyses of cortical and white matter masks were performed over a group of 25 newborns from 26 to 36 weeks of gestational age. Inter-individual variations associated with increasing age were first detected in large cerebral regions, with a prevalence of the right hemisphere in comparison with the left. Asymmetries were further highlighted in three specific cortical regions. Confirming previous studies, we observed deeper STS on the right side and larger posterior region of the sylvian fissure on the left side, close to planum temporale. For the first time, we also detected larger anterior region of the sylvian fissure on the left side, close to Broca's region. This study demonstrated that perisylvian regions are the only regions to be asymmetric from early on, suggesting their anatomical specificity for the emergence of functional lateralization in language processing prior to language exposure.

© 2010 Elsevier Inc. All rights reserved.

Introduction

During the last trimester of human pregnancy, the foetal brain undergoes major changes. Besides its critical and immense growth, its macroscopic morphology becomes greatly and quickly elaborated through the formation of sulci and gyri within the cortex. After a few months, the high complexity observed in the adult brain is already present, and sulcal patterns become variable across individuals (Ono et al., 1990). Additionally to its anatomical complexity, the adult cerebral hemispheres are asymmetric, notably through the "Yakovlevian torque" related to frontal and occipital petalias, and to the posterior shift in the sylvian fissure on the left compared with the right (Toga and Thompson, 2003).

Structural asymmetries were described early on in perisylvian regions. Heschl gyrus, planum temporale and superior temporal sulcus (STS) are asymmetric in the foetal and preterm brain (Chi et al., 1977b; Witelson and Pallie, 1973; Dubois et al., 2008a), and asymmetry in the sylvian fissure extent is progressively detected from adolescence to young adulthood (Sowell et al., 2002). Such asymmetrical structure is supposed to be closely related to the functional lateralization for language processing, which is already detected in the infant brain (Dehaene-Lambertz et al., 2006a). Nevertheless, direct correlations between anatomical and functional asymmetries are still lacking, since comparative *in vivo* measurements are then required.

Actually, specific early brain changes and asymmetries have been described many years ago in *post-mortem* brains (Feess-Higgins and Laroche, 1987). Recent advances in magnetic resonance imaging (MRI) enabled the study of such processes non-invasively, quantitatively and in three dimensions (3D) in the neonate. But imaging and mapping the cortical development in foetuses still remain a challenge without sedation because of foetal and maternal motion (Scifo et al., 2003). Studying the preterm newborn brain with dedicated post-processing tools (Hüppi et al., 1996; Cachia et al., 2003) has recently offered the opportunity to explore the early normal mechanisms of sulcation and gyrification (Dubois et al., 2008a) as well as disturbed processes and their functional significance (Dubois et al., 2008b). In particular, the folding of

* Corresponding author. CEA/SAC/DSV/DRM/NeuroSpin/Cognitive Neuroimaging Unit, Bât 145, point courrier 156, 91191 Gif-sur-Yvette, France. Fax: +33 1 69 08 79 73.
E-mail address: jessica.dubois@centraliens.net (J. Dubois).

1053-8119/$ – see front matter © 2010 Elsevier Inc. All rights reserved.
doi:10.1016/j.neuroimage.2010.03.054

major sulci has been quantified and time-scaled, and a rightward asymmetry of the STS has been detected (Dubois et al., 2008a).

Despite the provided breakthroughs, these studies presented the drawback of focusing on major identified sulci and disregarding other cortical regions, the anatomical localization of which may be hard to delineate among individuals. In this cross-sectional study, we aimed to blindly and automatically map local inter-hemispherical asymmetries over the whole preterm brain. We implemented a voxel-based approach, taking no a priori hypothesis on anatomical localization, in order to analyse cortical and white matter masks over a group of twenty-five newborns.

Materials and methods

Subjects

Twenty-five preterm newborns were included in this study (13 boys, 12 girls; mean gestational age – GA – at birth: 30.3 ± 2.5 weeks, range: 25.6–35.6 weeks; mean weight at birth: 1507 ± 514 g, range: 850–2730 g). This cohort of newborns has already been presented as the "normal groups" of previous publications (Dubois et al., 2008a,b; see Table 1 for details). The events around premature birth included risk of infection (maternal fever, increased white cell count and C-reactive protein CRP), premature rupture of membranes (PROM), placental abruption, preeclampsia and foetal distress (tachycardia, bradycardia, pathological cardiotocography CTG). No reason was found for three newborns. Seven newborns were intubated at birth, and the duration of ventilation ranged between 1 and 4 days. Fifteen newborns required continuous positive airway pressure (CPAP), for a time period ranging between 1 and 44 days. Table 1 summarizes these clinical details for all newborns.

All newborns were from singleton pregnancies and had a normal intra-uterine growth. Intra-uterine growth restriction (IUGR) was defined as birth weight below the 10th percentile for gestational age and gender and on criterion of placental insufficiency according to intra-uterine growth assessment, pre-natal ultrasound and Doppler measurements within the umbilical artery (see Tolsa et al., 2004; Dubois et al., 2008b).

The MRI examination (one per newborn) was performed as soon as possible after birth (mean GA at MRI: 31.5 ± 2.4 weeks, range: 26.6–35.7 weeks; mean time interval between birth and MRI: 1.2 ± 0.7 weeks, range: 0.1–3 weeks). The newborns' parents gave written informed consent for the study and the protocol was approved by the local ethical committee. The collection of all MRI data was performed within a time period of 4.9 years.

A radiologist specialized in neuro-pediatrics reviewed all MRI examinations acquired at birth and also at term-equivalent age. For all newborns, no lesion or cerebral abnormalities, in respect to their gestational ages, were detected on inversion recovery T1-weighted images, on T2-weighted images nor on diffusion-weighted images (maps of averaged diffusion coefficient ADC).

Data acquisition

During MR imaging, no sedation was used and the newborns were spontaneously asleep. Special "mini-muffs" were applied on their ears to minimize noise exposure. The study was conducted on a 1.5-T MRI system: Philips Medical Systems (Eclipse for 3 newborns, Intera for 12 newborns, Achieva for 1 newborn) or Siemens Medical System (Avanto for 9 newborns). The repartition of MRI systems among newborns is detailed in Table 1. Note that there was no relationship between the systems used and the babies' ages: the four systems were equally distributed with age.

Table 1
Clinical details for the 25 preterm newborns: Are presented, for each newborn.

No.	Gender	GA at MRI (weeks)	GA at birth (weeks)	Delay birth MRI (weeks)	MRI system	Events around premature birth	Birth weight (g)	Intubation	Ventilation (days)	CPAP (days)
1	F	26.6	25.6	1.0	Intera	No reasons for premature birth. Down way. Hypotension, respiratory distress syndrome.	950	No	0	42
2	F	27.9	26.6	1.3	Intera	Infectious risk (maternal febrile state, CRP increase). Caesarian.	850	No	0	12
3	F	28.1	27.1	1.0	Avanto	Foetal suffering and maternal febrile state. Caesarian.	1010	Yes	1	44
4	M	28.6	26.7	1.9	Avanto	PROM, maternal inflammatory syndrome. Down way.	990	No	0	1
5	F	29.6	28.3	1.3	Intera	Tachycardia and infectious risk (maternal febrile state and white cell increase). Caesarian.	900	Yes	3	43
6	F	29.9	28.4	1.4	Intera	PROM, infectious risk. Foetal suffering. Caesarian.	1140	No	0	2
7	F	30.0	28.7	1.3	Avanto	PROM, infectious risk (maternal white cell increase). Down way.	1280	No	0	31
8	M	30.3	30.0	0.3	Intera	Placental abruption and preeclampsia. Caesarian.	1600	No	0	0
9	F	30.4	29.9	0.6	Intera	Foetal pathological CTG traces, maternal uterine spasms. Caesarian.	1630	No	0	7
10	F	30.6	29.6	1.0	Avanto	Foetal pathological CTG traces. Caesarian.	1020	No	0	18
11	F	30.7	29.9	0.9	Avanto	Threat of premature birth. Down way.	1620	No	0	3
12	F	31.0	29.0	2.0	Intera	PROM and maternal CRP increase. Caesarian.	1090	No	0	1
13	F	31.1	30.7	0.4	Avanto	Placenta abruption, preeclampsia and foetal pathological traces. Caesarian.	1410	Yes	1	0
14	M	31.1	30.7	0.4	Avanto	Foetal suffering. Caesarian. Respiratory distress syndrome.	1330	No	0	0
15	M	32.0	29.9	2.1	Avanto	Preeclampsia. Caesarian.	1040	No	0	7
16	M	32.1	31.1	1.0	Avanto	Placental abruption and preeclampsia suspicion. Caesarian.	1370	Yes	1	7
17	M	32.6	30.4	2.1	Eclipse	PROM, maternal inflammatory syndrome. Caesarian	1590	No	0	0
18	M	33.3	31.6	1.7	Intera	Placental abruption and foetal bradycardia. Caesarian.	1735	Yes	2	2
19	M	33.6	30.6	3.0	Eclipse	No reasons for premature birth, no foetal suffering. Down way.	1800	No	0	0
20	F	33.7	32.4	1.3	Eclipse	PROM, maternal inflammatory syndrome. Down way.	1770	No	0	0
21	M	34.4	32.4	2.0	Intera	PROM, maternal inflammatory syndrome, oligoamnios. Caesarian. Asphyxia.	1980	Yes	4	0
22	M	34.4	33.3	1.1	Intera	PROM, maternal inflammatory syndrome. Caesarian.	2050	No	0	0
23	M	34.4	34.1	0.3	Intera	No reasons for premature birth, no foetal suffering. Down way.	2350	No	0	0
24	M	35.0	34.1	0.9	Achieva	Placental abruption. Caesarian.	2440	Yes	3	6
25	M	35.7	35.6	0.1	Intera	Foetal pathological CTG traces. Down way.	2730	No	0	0

Presented, for each newborn, the gender, the gestational ages (GA) at MRI and at birth, with time delay (in weeks), the MRI system used, the events around premature birth (CRP: Creactive protein, PROM: premature rupture of membranes, CTG: cardiotocography), birth weight (in grams), the need for intubation and the duration of ventilation (in days), and the need for continuous positive airway pressure (CPAP in days).

Please cite this article as: Dubois, J., et al., Structural asymmetries of perisylvian regions in the preterm newborn, NeuroImage (2010), doi:10.1016/j.neuroimage.2010.03.054

Coronal slices covering the whole brain were imaged by a 3D T1-weighted fast gradient recovery sequence and by a T2-weighted fast spin echo (FSE) sequence. With the Philips systems, a receive head coil was used and the acquisition parameters were: spatial resolution $0.7\times0.7\times1.5$ mm^3 (field of view FOV = 18×18 cm^2, matrix = 256×256), 80 coronal slices; no parallel imaging; T1-weighted sequence (fast field echo FFE): flip angle = 25°, 2 averages, for Eclipse TE/TR = 4/15 ms, for Intera/Achieva TE/TR = 4.2/13 ms; T2-weighted sequence: echo train length ETL = 16, for Eclipse TE/TR = 156/4040 ms, for Intera/Achieva TE/TR = 150/4000 ms.

For the Siemens system, a knee coil was used and the acquisition parameters were: spatial resolution $0.8\times0.8\times1.2$ mm^3 (FOV = 20×20cm^2, matrix = 256×256); parallel imaging GRAPPA factor 2; T1-weighted sequence (magnetized prepared rapid gradient echo MPRAGE): 96 coronal slices, flip angle = 9°, TE/TR/TI = 3.04/2200/1100 ms; T2-weighted sequence: 84 coronal slices, ETL/Turbo factor = 15, TE/TR = 151/5700 ms.

Data post-processing

Individual segmentations

We focused on processes happening in the cortex and in the subcortical white matter. For each newborn, these tissues were segmented by two independent methods, which enabled to increase the results reliability. The post-processing methodologies were dedicated to the preterm newborn brain because of the different contrast in immature cerebral tissues on T1- and T2-weighted images compared with the adult brain.

With the first method, cerebral tissues were segmented using an optimal non-parametric density estimator with k-nearest neighbour (KNN) classification, based on the MR signal intensity of the registered T2- and T1-weighted images and on anatomic location (Hüppi et al., 1998; Warfield et al., 2000; Inder et al., 2005). The mask of cortex was delineated with this method (see Fig. 2).

With the second method, the interface between cortex and white matter was segmented coherently in 3D using a semi-automatic sequence of image post-processing tools based on mathematical morphology and thresholding of the T2-weighted images (Dubois et al., 2008a; Cachia, et al., 2003; Mangin et al., 2004). This method generated the mask of white matter, but did not enable to exclude the central grey nuclei from this mask in the medial surface (see Fig. 2). It was not problematic as we were focused on inter-individual variations and inter-hemispheric asymmetries localized at the interface between cortex and white matter.

Images preparation for voxel-based analyses

For image normalization and voxel-based analyses, Statistical Parametric Mapping software was used (SPM5, FIL, http://www.fil.ion.ucl.ac.uk/spm/).

A template of T2 images, which took into account inter-hemispherical asymmetries, was created over the 25 newborns by two successive steps (Watkins et al., 2001). A targeted newborn was first selected based on its mean age (31.1 weeks) corresponding to an intermediate cortical sulcation and on its regular head shape. Its T2 images were aligned in the plane of anterior/posterior commissures (AC/PC plane). Second, for all newborns, T2 images and T2 images flipped on the left-right axis were normalized non-linearly to these newborn images. The T2 template was created by averaging the 50 resulting images.

For voxel-based analyses, the T2 images of each newborn, flipped or not flipped (native), were normalized to the template, and the resulting normalization transformation was applied to the individual masks of cortex and white matter, flipped or not flipped. Asymmetry maps between the normalized native (N) and flipped (F) images $(N-F)/(N+F)$ were calculated for each newborn. All images were smoothed with a 3-mm Gaussian filter. This filter size was chosen according to the small size of cerebral structures in preterm newborns and to the image spatial resolution.

Analyses of inter-individual variations associated with increasing age and analyses of inter-hemispherical asymmetries

The independent analyses of cortex and white matter masks are expected to provide equivalent results. Inter-individual variations associated with increasing age can be simplified in terms of image voxels labelling (Fig. 1). Where a cortical sulcus folds, the underlying white matter is spatially shifted and replaced in appearance by grey matter. Then voxels labelled as white matter for the youngest newborns are labelled as cortex in the edges and bottoms of the sulcus for the oldest newborns. This led to an "apparent increase" in cortex and an "apparent decrease" in white matter (it is not a "true decrease" but a spatial shift). In the current cross-sectional study, the corresponding voxels were realigned across newborns of different ages. In the same way, asymmetries in cortex correspond to opposite asymmetries in white matter.

Fig. 2 summarizes the pipeline of analyses. The inter-individual variations in the masks of cortex and white matter associated with increasing age were evaluated using voxel-based linear regressions with gestational age at MRI as covariate. Asymmetries between cerebral hemispheres in the localization of cortex and white matter were evaluated by testing the nullity of asymmetry maps over the group with a one-tailed paired *t*-test on a voxel-by-voxel basis.

We further evaluated the role of the sex on inter-individual variations and asymmetries by adding this parameter as a supplementary covariable in the analyses. The influence of age on asymmetries was also assessed.

The mask of analyses included the cerebrum and excluded the cerebellum. Statistical thresholds were considered at the voxel level at $p_{\text{FDR-corr}}<0.05$ after correction for multiple comparisons with "false discovery rate" (FDR) approach. In the Results section, we only presented clusters with $p_{\text{corr}}<0.001$ at the cluster level. This approach excluded clusters smaller than 157 and 223 voxels for age-associated variations in cortex and white matter and clusters smaller than 33 and 15 voxels for asymmetries in cortex and white matter.

For all analyses, clusters of the internal cortical surface are presented in the tables but are not detailed in the text because individual segmentations were fairly reliable there, close to the inter-hemispheric fissure and the central grey nuclei (see Dubois et al., 2008a).

Results visualization

In order to provide a basis for the results visualization, an averaged symmetrical inner cortical surface was generated in 3D (Fig. 3). To do so, the normalized native and flipped masks of white matter were averaged over the 25 newborns, providing a probability map. Before computing a smooth triangle-based mesh, this map was

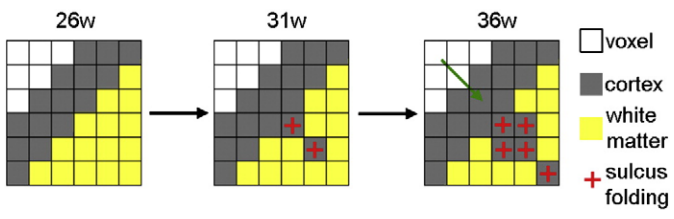

Fig. 1. Schema of sulcus folding: The schema outlined the inter-individual variations associated with increasing age (e.g. at 26, 31 and 36 weeks of gestational age) in terms of image voxels labelling. Where a sulcus folds (red crosses), voxels labelled as white matter (in yellow) for the youngest newborns became labelled as cortex (in grey) in the edges and bottoms of the sulcus for the oldest newborns. This led to an "apparent increase" in cortex and an "apparent decrease" in white matter. Such observations were performed cross-sectionally in the current study. Because of the time interval and of the insufficient spatial resolution compared with the cortical thickness, the gradual hollow between the two sulcus sides (green arrow) is not visible.

Please cite this article as: Dubois, J., et al., Structural asymmetries of perisylvian regions in the preterm newborn, NeuroImage (2010), doi:10.1016/j.neuroimage.2010.03.054

ARTICLE IN PRESS

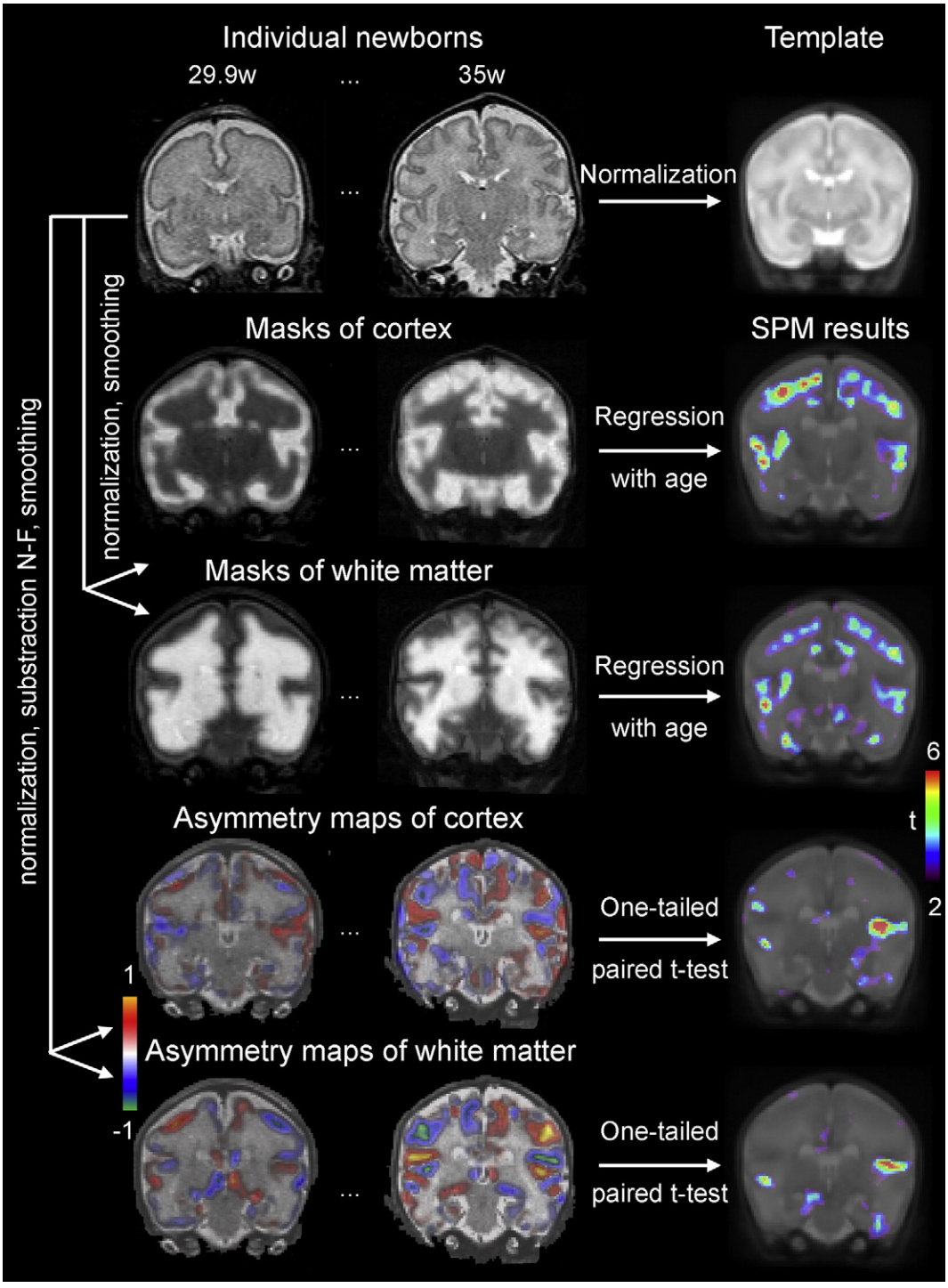

Fig. 2. Pipeline of analyses: Individual T2 images (examples here for preterm newborns of 29.9 and 35 weeks old) were normalized to the newborn template (1st line). The corresponding normalizations were applied to the masks of cortex and white matter, and the SPM group analyses outlined age-associated variations by linear regression (2nd and 3rd lines). Asymmetry maps were generated by the subtraction of normalized native and flipped masks, and the SPM group analyses outlined inter-hemispherical asymmetries by one-tailed paired *t*-test (4th and 5th lines).

thresholded and two successive steps of erosion and dilation were further applied. Thresholding the probability map for a threshold T is equivalent to consider the voxels of white matter masks present in at least Tx25 newborns. Because of inter-individual variability, the choice for threshold T influences the resulting averaged surface, so different thresholds were tested (Fig. 3). For lowest thresholds (e.g. $T=0.4/0.6$), many voxels are kept by this procedure, and the averaged surface is smoothed, without sufficient sulci folding (see for instance the sylvian fissure and the central sulcus). On the contrary, for highest thresholds (e.g. $T=0.9$), only voxels present in all newborns are kept, and the sulci of the averaged surface are too shallow (see for instance the superior temporal sulcus). The resulting averaged surface appeared the most visually correct, with a coherent folding of cortical sulci, for an intermediate threshold $T=0.8$ (see Fig. 3). It then looked like an individual cortical surface of a 29-week-old newborn. The choice for threshold T may seem arbitrary, but it was only useful for results visualization and did not influence the results of analyses.

Please cite this article as: Dubois, J., et al., Structural asymmetries of perisylvian regions in the preterm newborn, NeuroImage (2010), doi:10.1016/j.neuroimage.2010.03.054

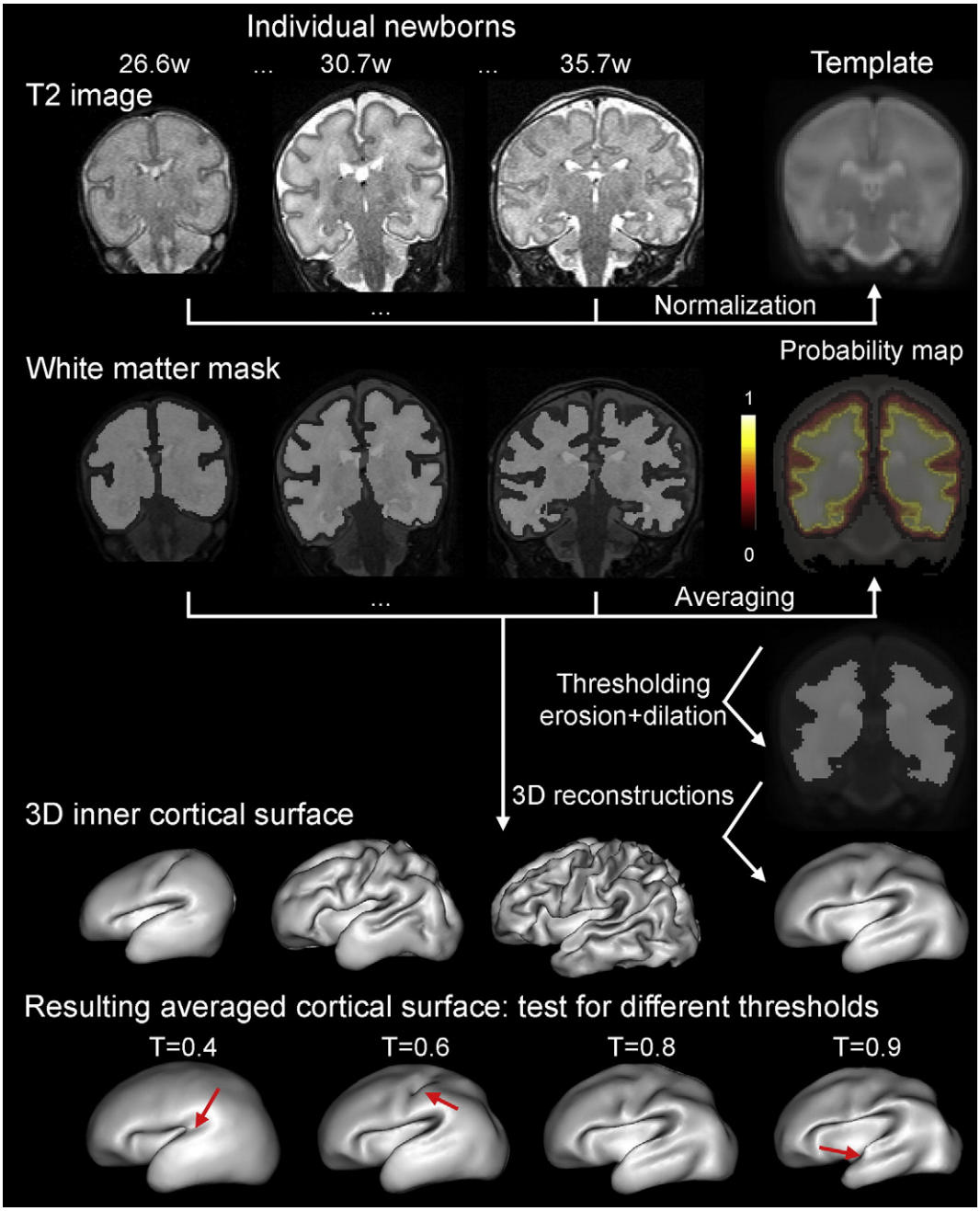

Fig. 3. Creation of the 3D averaged inner cortical surface: Individual T2 images (examples here for preterm newborns of 26.6, 30.7 and 35.7 weeks old) were normalized to the newborn template (1st line). The corresponding normalizations were applied to the masks of white matter, and the resulting native and flipped masks were averaged to create the probability map of white matter (2nd line). This map was thresholded, eroded and dilated to provide a mask for the 3D averaged inner cortical surface (3rd and 4th lines). Different thresholds were tested (5th line). For small thresholds ($T=0.4/0.6$), the averaged surface is smoothed, without enough sulci folding (arrows at the level of the sylvian fissure and central sulcus). For high threshold ($T=0.9$), the sulci of the averaged surface are too shallow (arrow at the level of the superior temporal sulcus). An intermediate threshold ($T=0.8$) seemed a good compromise to provide a visually correct averaged surface, with a coherent folding of cortical sulci. This surface looked like an individual cortical surface of a 29-week-old newborn.

Statistical results from the voxel-based analyses were projected on this averaged inner cortical surface by considering the mean *t*-values over a sphere of 1 mm radius around each point of the surface mesh. This radius was chosen according to the image spatial resolution. Such a projection was more robust than a simple "point-to-point" projection.

For visualization purposes, the results clusters were also projected on the individual cortical surfaces of the four oldest newborns (GA: 34.4–35.7 weeks old), who presented the greatest and most sophisticated patterns of sulcation. These projections enabled the qualitative comparison of the localization of individual cortical sulci, when present, and the clusters showing inter-individual variations or inter-hemispherical asymmetries. To do so, only the linear part of the normalization transformation was applied to the cortical surface of each newborn in order to keep the surface spherical topology (Dubois et al., 2008a).

Results

As previously detailed (Dubois et al., 2008a), the post-processing of high quality T1- and T2-weighted images, free from motion artifacts, enabled the segmentations of cortex and white matter in

Please cite this article as: Dubois, J., et al., Structural asymmetries of perisylvian regions in the preterm newborn, NeuroImage (2010), doi:10.1016/j.neuroimage.2010.03.054

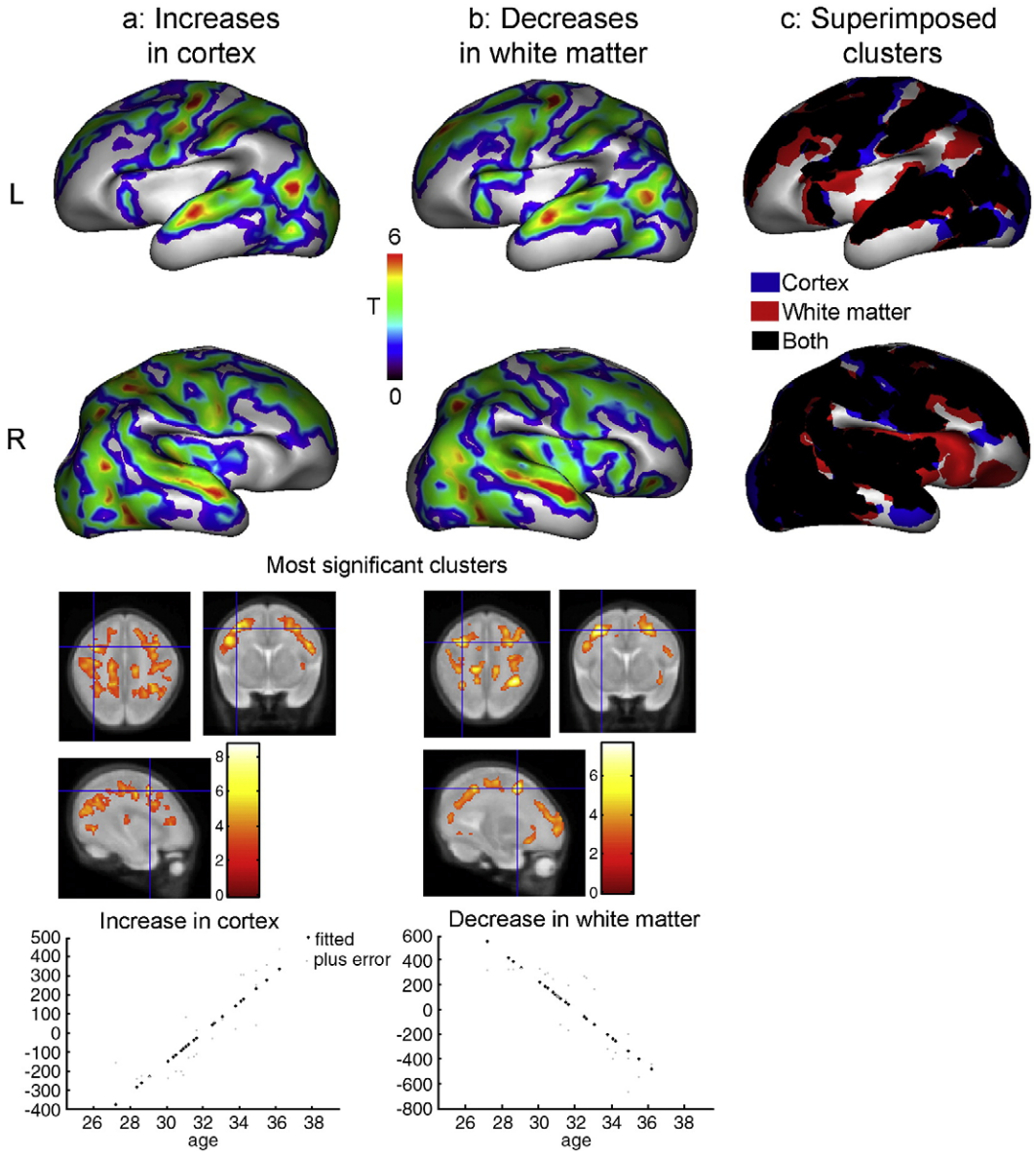

Fig. 4. Inter-individual variations associated with increasing age in the preterm group: In the first two rows, statistical T-maps are superposed to the 3D averaged cortical surface in the significant clusters showing "apparent increases" in cortex (a) and "apparent decreases" in white matter (b), for the left (L, up) and right (R, down) hemispheres. The clusters (c) for cortex (blue) and white matter (red) are mainly overlying (black). Note that the right hemisphere shows larger regions of age-associated variations in comparison with the left hemisphere. In the third row, statistical T-maps are presented in 2D, with cursors on the most significant clusters. The last row shows the plots of "apparent increase" in cortex and "apparent decrease" in white matter associated with increasing age and measured in these clusters (fitted signals plus errors).

each preterm newborn brain by using two independent methods. The contrast in the images and the quality of segmentations were equivalent across all newborns and MRI systems.

Inter-individual variations associated with increasing age

Inter-individual variations in cortex and white matter were associated with increasing age quantitatively and spatially with voxel-based analyses over the whole 25 newborns. "Apparent increases" in cortex (Fig. 4a) and "apparent decreases" in white matter (Fig. 4b) were demonstrated in large regions across both hemispheres of the brain (Table 2), in the places of sulci folding (see Fig. 1). Sex had no influence on these variations.

In the left hemisphere, statistical peaks were observed for the cortex in the temporal anterior, temporo-occipital and pre-central regions. For white matter, peaks were detected at the level of the temporal anterior, temporo-occipital, pre-central superior and frontal anterior regions. In the right hemisphere, peaks were located for the cortex in the superior temporal sulcus (STS), the temporo-occipital, parietal and superior post-central regions. For white matter, peaks were at the level of the STS, the temporo-occipital, parietal and frontal inferior regions.

The clusters detected in the analyses of cortex and white matter mainly overlaid (Fig. 4c), confirming that the two independent methods provided equivalent information. For both tissues, the significant clusters were larger in the right (R) hemisphere in comparison with the left (L) hemisphere (cortex: R 12654 voxels/L 11955 voxels; white matter: R 13405 voxels/L 12575 voxels), suggesting that inter-individual variations associated with increasing age are more intense on the right side over this preterm age period.

These age-associated variations were mostly related to the folding of cortical sulci rather than to cortical thickening or to changes in gyri or sulci positions and shapes. In fact, a growing sulcus corresponded to the "apparent emergence" of cortex in specific voxels, going with a "spatial shift" of underlying white matter (see Fig. 1). In order to confirm this hypothesis, the clusters intersecting for both analyses of cortex and white matter were further projected on the most folded

Please cite this article as: Dubois, J., et al., Structural asymmetries of perisylvian regions in the preterm newborn, NeuroImage (2010), doi:10.1016/j.neuroimage.2010.03.054

Table 2
Voxel-based analyses of inter-individual variations associated with age in the preterm group.

Cluster	Localization	Cluster level: no. voxels	Voxel level: *t*-value ($p_{FDR\text{-}corr}$)
Cortex increase with age			
1	L temporal anterior/temporo-occipital/pre-central regions	11955	8.70 (0.001)
2	R STS/temporo-occipital/parietal/ superior post-central regions	12654	7.32 (0.002)
White matter decrease with age			
1	L pre-central region/frontal anterior/ temporal anterior	11280	7.61 (0.001)
2	R STS/parietal region	8444	7.59 (0.001)
3	R frontal inferior region	353	7.08 (0.001)
4	R temporal inferior region	362	6.20 (0.002)
5	R frontal anterior/pre-central regions	4246	5.65 (0.003)
6	L occipital regions	902	5.38 (0.005)
7	L insula anterior regions	393	4.91 (0.007)

Voxel-based analyses of inter-individual variations associated with age in the preterm group: The statistically significant clusters for inter-individual variations associated with increasing age ($p_{FDR\text{-}corr}<0.05$ at the voxel-level, $p_{corr}<0.001$ at the cluster-level) are outlined in order of significance, with their localization (in the left (L) and right (R) hemispheres), number of voxels, t value at local maxima, and in parenthesis p value after correction for multiple comparisons with FDR approach. An "apparent increase" in cortex and an "apparent decrease" in white matter are associated with increasing age.

cortical surfaces of four individual newborns, and their localization was qualitatively compared with the sulci localization (Fig. 6). These projections showed that clusters were mostly located in the sulci floors in the left hemisphere, whereas right clusters appeared to be more diffuse. Small discrepancies can be observed among newborns in the clusters localization. These are inherent to the projection procedure, which did not take into account the non-linear components of the images' normalization.

Inter-hemispherical asymmetries

In comparison with the analyses of inter-individual variations, the analyses of inter-hemispheric asymmetries outlined more specific clusters (Table 3). Some regions presented asymmetries in cortex (Fig. 5a) and/or white matter (Fig. 5b). The side of the presented clusters corresponds to the place where an "apparent excess" in cortex or an "apparent lack" in white matter was detected in comparison with the controlateral region. Sex, gestational age at MRI or post-natal age (maximal 2 weeks) had no influence on these asymmetries.

Table 3
Voxel-based analyses of inter-hemispherical asymmetries in the preterm group.

Cluster	Localization	Cluster level: no. voxels	Voxel level: *t*-value ($p_{FDR\text{-}corr}$)
Asymmetries in cortex			
1	L posterior insula region	314	10.01 (<0.001)
2	R frontal inferior region	82	6.08 (0.005)
3	R STS	63	6.05 (0.006)
4	L anterior insula region	109	5.98 (0.006)
5	L frontal medial region	99	5.69 (0.008)
Asymmetries in white matter			
1	R superior posterior insula region	82	6.89 (0.013)
2	L posterior insula region	327	6.66 (0.013)
3	L anterior insula region	161	5.97 (0.015)
4	R STS	69	5.70 (0.015)
5	L medial frontal region	152	5.62 (0.015)
6	R medial parieto-occipital region	51	5.58 (0.015)
7	R STS	51	5.54 (0.015)
8	R medial temporo-occipital region	25	5.04 (0.021)
9	R medial temporal region	29	4.94 (0.021)

Voxel-based analyses of inter-hemispherical asymmetries in the preterm group: The statistically significant clusters for inter-hemispherical asymmetries ($p_{FDR\text{-}corr}<0.05$ at the voxel-level, $p_{corr}<0.001$ at the cluster-level) are outlined in order of significance, with their localization, number of voxels, t value at local maxima, and in parenthesis p value after correction for multiple comparisons with FDR approach. The indicated region, in the left (L) or right (R) hemisphere, presents a higher proportion in cortex or a lower proportion in white matter in comparison with its controlateral region.

For both tissues, asymmetries were detected in the right STS and the left anterior and posterior regions of sylvian fissure—bordering Broca's region and the planum temporale. A superior posterior region of the sylvian fissure was also detected for white matter in the right hemisphere. Again, the results provided by the methods based on cortex and white matter were particularly congruent (Fig. 5c).

The clusters projection on the individual cortical surfaces with greatest folding enabled to precise their anatomical localization (Fig. 6). The right STS cluster seemed located at the level of the sulcus inferior edge rather than at the sulcus floor. Left clusters edged the sylvian fissure, bordering, in the anterior side, the pars triangularis of the inferior frontal gyrus, and, in the posterior side, the planum temporale.

Discussion

In this study, we described inter-hemispherical asymmetries *in vivo* in the premature brain in terms of inter-individual variations associated with increasing age, folding and local geometry. To do so, we used automatic voxel-based analyses of cortical and white matter masks over a group of 25 newborns, from 26 to 36 weeks of gestational age.

The age-associated variations mostly corresponded to the emergence of cortical sulci given their localization. Where a sulcus folds, voxels that are labelled as white matter in the youngest newborns are labelled as cortex in the oldest newborns. When regression with gestational age is performed, it implies an "apparent increase" in cortex and an "apparent decrease" in white matter over the folding time period. We probably did not detect variations in cortical thickness; otherwise, their localization would have been more uniform across the whole cortex and not specifically focused around the sulci (see Fig. 6). With this approach and non-linear normalization, we did not detect variations neither in the positions of cortical sulci and gyri nor in their "winding" shapes (shapes with equivalent sizes and depths). Otherwise, we would also have detected neighbour voxels with opposite inter-individual variations, showing both cortical "apparent decrease" and white matter "apparent increase".

From 26 to 36 weeks of gestational age, inter-individual variations were observed in large regions across the brain (pre- and post-central, temporal, frontal and parieto-occipital), which is coherent with *post-mortem* and pre-natal studies of foetal brains (Feess-Higgins and Laroche, 1987; Chi et al., 1977a; Garel et al., 2001). Larger variations were detected over the right hemisphere in comparison with the left. It probably relies on the earlier gyral complexity of this hemisphere: previous *post-mortem* observations actually described that right sulci appear before left ones by two weeks (Chi et al., 1977b). Regions with the most acute variations over this age range are to be the first cortical places to fold, as well as the most spatially stable regions across individuals. It may represent the "sulcal roots" (Regis et al., 2005) from where the primary sulci fold (Lefèvre et al., 2009). In this perspective, it would be interesting to further compare the localization of our age-related clusters in the preterm brain with the deepest sulcal pits identified in the adult brain (Im et al., 2010). Nevertheless, the huge differences in brain morphology between preterm newborns and adults would make the registration tough and problematic.

In addition to inter-individual variations associated with increasing age, local inter-hemispherical asymmetries were detected in three specific regions around the sylvian fissure. These asymmetries affected the cortex, as the current methodology did not enable to study asymmetries in internal white matter.

The STS appeared deeper on the right side, coherently with previous results in *post-mortem* foetuses (Chi et al., 1977b), *in vivo* preterm newborns (Dubois et al., 2008a) and adults (Van Essen, 2005). Based

Please cite this article as: Dubois, J., et al., Structural asymmetries of perisylvian regions in the preterm newborn, NeuroImage (2010), doi:10.1016/j.neuroimage.2010.03.054

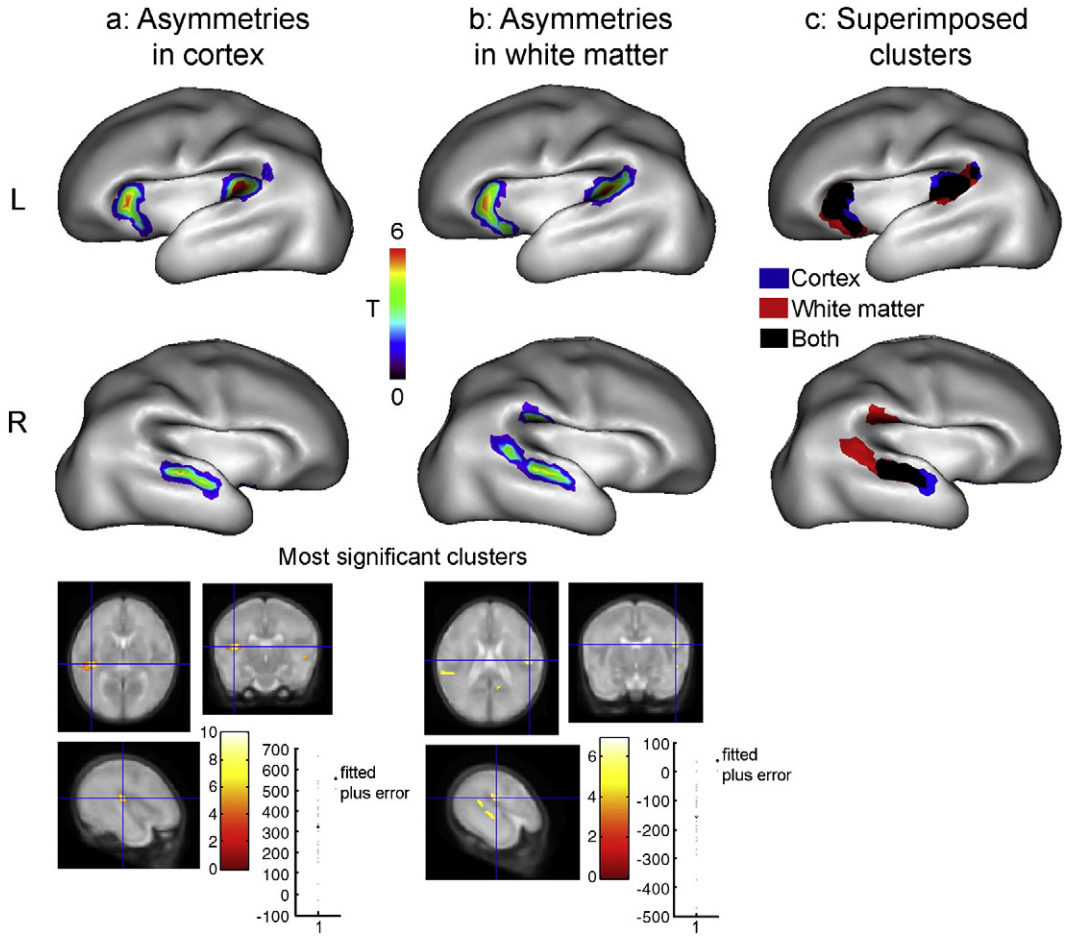

Fig. 5. Inter-hemispherical asymmetries in the preterm group: In the first two rows, statistical T-maps are superposed to the 3D averaged cortical surface in the significant clusters showing asymmetries in cortex (a) and white matter (b), for the left (L, up) and right (R, down) hemispheres. The clusters (c) for cortex (blue) and white matter (red) are mainly overlying (black). In the third row, statistical T-maps are presented in 2D, with cursors on the most significant clusters, where the plots of asymmetry in cortex and white matter were measured (fitted signals plus errors).

only on these structural observations, it was not possible to conclude whether this sulcus asymmetry is related to an advanced functional maturation of the right cortical region. It is interesting to note that this STS region has also been identified as asymmetrical in the adult brain according to the frequency and spatial distribution of sulcal pits (Im et al., 2010), given the absence of pits cluster in the right hemisphere. This seems contradictory with our observation of higher depth on the right side in the preterm brain, and with the hypothesis that sulcal pits of the adult brain and sulcal roots of the developing brain may correspond to each other (Cachia et al., 2003).

Besides the STS asymmetry, two anterior and posterior regions of the sylvian fissure seemed larger on the left side, close to Broca's region and planum temporale. This may suggest that the development of these regions is in advance on the left side. We rather believe that the structural morphology of these regions is intrinsically different across both hemispheres, from early on.

Actually, previous studies have described that planum temporale is larger in the left hemisphere of foetal and newborn brains, as in the adult brain (Geschwind and Levitsky, 1968; Witelson and Pallie, 1973; Wada et al., 1975; Chi et al., 1977b, Galaburda et al., 1978). Additionally, the adult sylvian fissure is longer on the left side with a shorter and steeper right posterior extent (Lyttelton et al., 2009), and this asymmetry increases from childhood to young adulthood (Sowell et al., 2002). Given the characteristics of our realignment method, which will be discussed below, the posterior asymmetry of sylvian fissure that we detected in preterm newborns may rather correspond to the planum temporale asymmetry than to the sylvian fissure shift.

Cytoarchitectonic asymmetries in Broca's region have been found to increase with age, during infancy and childhood, from 1 year of age (Amunts et al., 2003). In the adult brain, morphological asymmetries are controversial and not reproducibly demonstrated across studies (Keller et al., 2009), maybe because the sulcal contours of this region are variable. Since these anatomical landmarks are lacking in preterm newborns, we could not conduct further analysis to validate that the asymmetrical region detected in the anterior sylvian fissure belongs to Broca's region.

Interestingly, apart from these three perisylvian regions, no other cortical regions appeared asymmetric on the external cortical surface of preterm newborns. First, we confirmed previous *post-mortem* and *in vivo* studies for the prevalence of the right STS and left planum temporale. Second, we detected for the first time an additional perisylvian region, close to Broca's region. This asymmetry may have never been reported before because of the lack of anatomical landmarks bordering the region, which required the use of a voxel-based approach. The absence of other asymmetries brings out the reliability and specificity of our results.

These three perisylvian regions are known to play a major role in the speech perception and production in the adult brain. In this perspective, we previously studied a cohort of healthy infants, from 1 to 4 months of age, and demonstrated that the arcuate fasciculus, which connects the cortical regions of the speech perisylvian network, is the most asymmetrical region of the developing white matter (Dubois et al., 2009). With diffusion tensor imaging, we demonstrated that this fasciculus is larger and more posterior in the left temporal

Please cite this article as: Dubois, J., et al., Structural asymmetries of perisylvian regions in the preterm newborn, NeuroImage (2010), doi:10.1016/j.neuroimage.2010.03.054

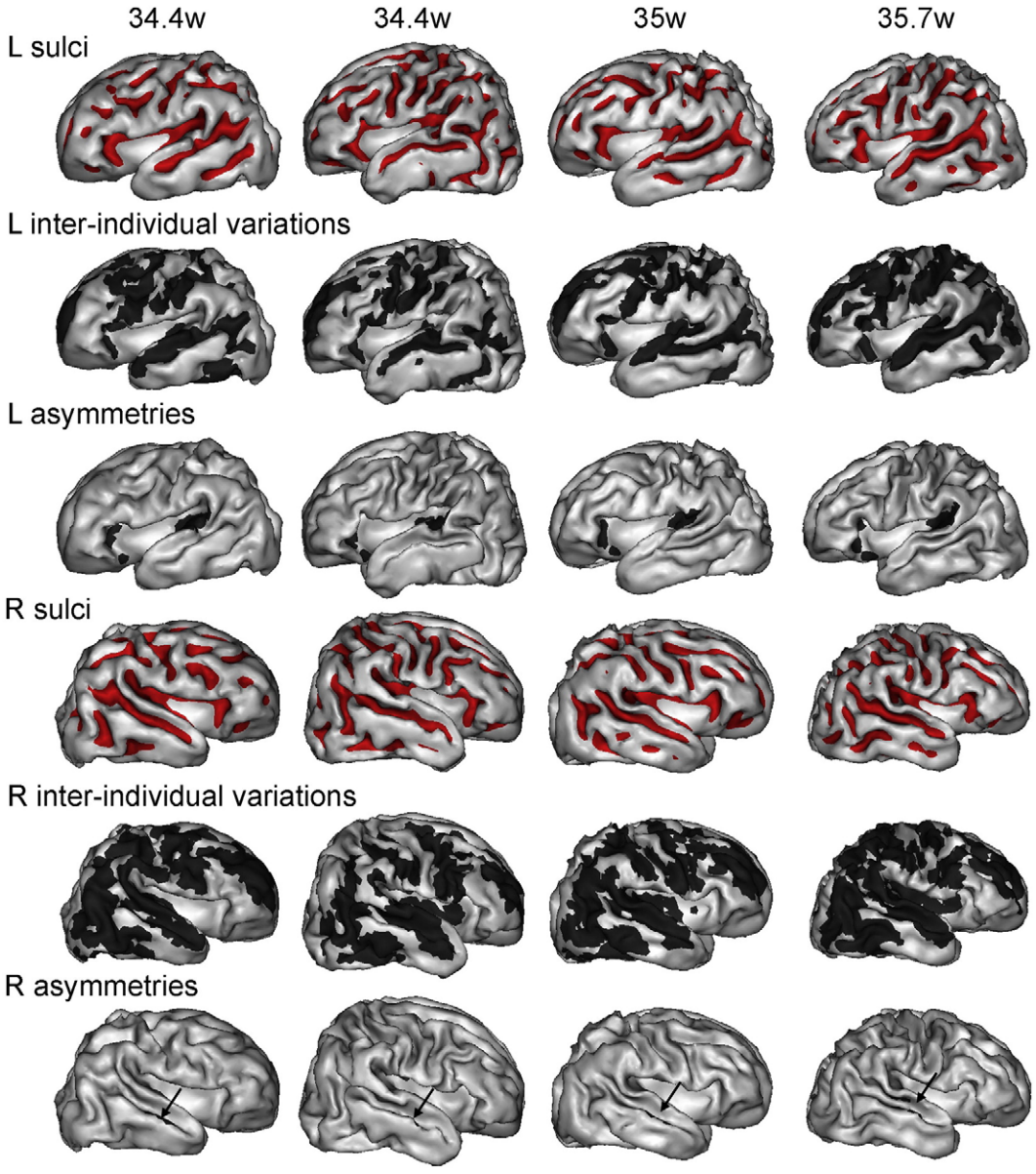

Fig. 6. Individual localization of cortical sulci, inter-individual variations associated with increasing age and inter-hemispherical asymmetries in four newborns: In the first and fourth lines, the left (L) and right (R) individual cortical surfaces of the four oldest newborns (GA: 34.4–35.7 weeks old) highlight the sulci localization in red (corresponding to a negative curvature of the surface). These newborns present a great sulcation pattern compared with the younger newborns. For both analyses (age-associated variations: second and fifth lines; inter-hemispherical asymmetries: third and sixth lines), the intersections of clusters for cortex and white matter analyses (see Figs. 4c and 5c) are overlaid to these surfaces. Note that clusters for age-associated variations are mostly located in the folding sulci in the left hemisphere. The asymmetry cluster of the right STS is barely visible because of its localization in the sulcus inferior edge (arrow).

region, and more compact in the left parietal region, in agreement with adult observations (Buchel et al., 2004). It may seem contradictory to observe opposite asymmetries in the cortex (asymmetry favouring the right side at the level of the STS) and in the underlying white matter (asymmetry favouring the left side at the level of the arcuate fasciculus). Actually, these measurements were performed at different periods of development, with various exposures to language. Furthermore, a simplistic mechanical model may describe that these structures occupy opposite spatial volumes from one another, and that a larger fasciculus gives fewer places for the sulcus to fold.

In the current study, we did not find statistically significant relationships between the inter-hemispherical asymmetries and the newborns' age. This indicates that the asymmetries are present early on, even in the younger newborns. For instance, the STS develops earlier on the right side (Chi et al., 1977b), which implies that its asymmetry can be detected as soon as the sulcus folds. Nevertheless, by lowering the statistical thresholds ($p<0.01$ without correction for multiple comparisons), we observed that the asymmetries tend to increase with age.

The precocity of these anatomical asymmetries supports the hypothesis that the early structure of perisylvian regions is intrinsically and closely related to the development of functional lateralization for language in the infant brain (Dehaene-Lambertz et al., 2006a). In order to interrelate precisely anatomical and functional developments, additional *in vivo* studies of language processing are required in newborns (Dehaene-Lambertz et al., 2006b; Simon et al., 2009). Only joint analyses of anatomical and functional MRI will enable to determine the maturational and functional significance of anatomical asymmetries in the cortical and white matter perisylvian regions.

The inherent limitation of this study was the use of premature newborns, who may not be representative of normal neurodevelopment.

Please cite this article as: Dubois, J., et al., Structural asymmetries of perisylvian regions in the preterm newborn, NeuroImage (2010), doi:10.1016/j.neuroimage.2010.03.054

Because of the pregnancy events which triggered the premature birth and the early exposure to extra-uterine stimulations, these individuals born before term may differ in brain structure and developmental trajectories in comparison with normal foetuses, even if no gross MRI lesions were detected. In this perspective, extremely preterm infants show a decreased volume and a less complex surface of cortex at term-equivalent age (Ajayi-Obe et al., 2000; Inder et al., 2005; Kapellou et al., 2006). However, we here studied the preterm newborns only a few days after birth, and the secondary influence of extra-uterine development may be reduced. For practical reasons related to motion and acquisition time, studying normal foetuses with such high-resolution MRI is hardly feasible *in utero*. Nevertheless, this study might be considered thanks to new ultra-rapid acquisition schemes, movement corrections and dedicated post-processing tools (Rousseau et al., 2006; Jiang et al., 2007; Rutherford et al., 2008).

An additional limitation of this study is the cross-sectionality of the preterm data. For obvious ethical reasons, it was not possible to acquire longitudinal MRI data in the same newborns. Only two examinations were performed, soon after birth and at term-equivalent age in order to check the normality in brain development.

Given the difficulty to bring together a cohort of preterm newborns, this study lasted over 4.9 years. Therefore, it was not possible to guarantee the use of a single MRI system in our University Hospital, and imaging parameters slightly differed across newborns. Nevertheless, the spatial resolution was almost the same, the contrasts of T1- and T2-weighted images were equivalent and the quality of segmentations was high for all subjects. Using images obtained with different hardware did not impact the results of inter-hemispherical differences, as within-subject analyses were performed. On the contrary, it might affect the results of age-associated variations observed across subjects, if there was any consistent relationship between the systems used and the babies' age. Fortunately, this was not the case in the present study: newborns from all gestational ages were regularly included across years, and consequently there was an overlap between the Philips and Siemens systems across ages (see Table 1). This supported the assumption that our previous results were not biased by the use of images acquired from different MRI systems (Dubois et al., 2008a,b).

In this report, the investigations of inter-individual variations associated with age and inter-hemispherical asymmetries were conducted locally but over the whole brain, with an automatic method which did not require the anatomical delineation of structures. It enabled to map regions for which localization is hard to map. To our knowledge, it is the first time that this approach is used to quantify inter-individual and inter-hemispherical differences over this range of ages. In a recent study (Dubois et al., 2008a), we were able to evaluate sulci development by mapping them individually across preterm newborns, but it required a precise identification and labelling a priori before analysis. On the contrary, group analysis on a voxel-by-voxel basis here provided the possibility to "blindly" compare cortical development across newborns without focusing on a particular region or sulcus. This methodology enabled to detect for the first time *in vivo* a coherent inter-hemispherical asymmetry, close to Broca's region.

This approach required the implementation of a specific symmetrical MRI T2 template. The methodology was inspired from the initial study of Watkins et al. (2001), who detailed inter-hemispherical asymmetries in the adult brain. A 3D averaged reconstruction of cortical surface was further computed for results visualization.

Realigning together all preterm newborn brains was the first methodological issue that we encountered with the voxel-based approach. First, for the template implementation, we selected a targeted newborn of regular head shape and mean age corresponding to an intermediate cortical sulcation. A non-linear registration of individual T2 images to the template was used in order to deal with the differing head shapes and cortical sulcations with age. An affine registration was also tested, providing very similar results for voxel-based analyses of inter-individual variations and inter-hemispherical asymmetries (results not shown). Given the structural variability over the newborns, related to the presence or absence of secondary and tertiary sulci, one may be sceptical on the appropriateness of this approach to realign developing brains. However, one should remind that the sulcation of a 36-week preterm newborn is still far more simplified than the sulcation of a term (40 w) infant. Then realigning globally the brains was sufficient to roughly realign the sulci. Furthermore, in the youngest newborns (26 weeks of gestational age), only a few sulci were present (sylvian fissure and central sulcus on the external surface), which precluded the application of a surface registration based on sulci realignment (Van Essen, 2005) to our newborns group. In the future, the detection of more specific changes will require to group the newborns according to their gestational age. Unfortunately, in the present study, the small size of our cohort did not enable us to perform further statistical analyses in that case.

Our T2 template integrated macroscopic left-right asymmetries since it was the average of native and flipped normalized individual images. Such a template was necessary to detect local coherent asymmetries, and not global asymmetries related for instance to frontal and occipital petalias (Dubois et al., 2009).

Besides, to characterize cortical development, we analysed both the masks of cortex and white matter, after segmenting these tissues by two independent methods. We focused on the external surface of the cortex, because individual segmentations were fairly reliable at the level of the internal cortical surface, close to the inter-hemispheric fissure and the central grey nuclei (Dubois et al., 2008a). Detecting similar inter-individual variations and inter-hemispherical asymmetries for both cortex and white matter supported the reliability of our results.

For the calculation of asymmetry maps, we computed the ratio $(N-F)/(N+F)$, and not only the difference $(N-F)$, in order to be coherent with previous studies of asymmetries (Dubois et al., 2008a, 2009). In these studies, the normalization by the sum $N+F$ was required in order to take into account the inter-individual variability in cortical surface or diffusion anisotropy related to the different ages of newborns or infants. Here, the normalization by the sum $N+F$ did not change the value of the asymmetry because the considered masks only took two binary values (0 or 1).

In the future, this global approach with voxel-based analyses will be applied for group comparisons between preterm newborns experimenting different pre-natal environment (Dubois et al., 2008b) or receiving various post-natal treatments (Benders et al., 2009). It may enable the automatic detection of particularities or pathologies in the developing preterm brain according to gestational age at birth (Ajayi-Obe et al., 2000) or to functional outcome during childhood (Thompson et al., 2008). Finally, further correlations will be performed between anatomical asymmetries of perisylvian regions and functional activities in preterm and term newborns with various exposure times to language listening (Simon et al., 2009).

Acknowledgments

This work was supported by the Center for Biomedical Imaging (CIBM) of Geneva and Lausanne, by the Swiss National Foundation (grants nos. 32-56927, 3200B0-102127; PSH), by the Leenards Foundation (PSH), by the EU grant NEOBRAIN (www.neobrain.eu, grant no 036534; PSH) and by the French National Agency for Research (grant EPILEPSY_DEV/ANR-05-NEUR-014-01; JD).

References

Ajayi-Obe, M., Saeed, N., Cowan, F.M., Rutherford, M.A., Edwards, A.D., 2000. Reduced development of cerebral cortex in extremely preterm infants. Lancet 356, 1162–1163.

Amunts, K., Schleicher, A., Ditterich, A., Zilles, K., 2003. Broca's region: cytoarchitectonic asymmetry and developmental changes. J. Comp. Neurol. 465, 72–89.

Please cite this article as: Dubois, J., et al., Structural asymmetries of perisylvian regions in the preterm newborn, NeuroImage (2010), doi:10.1016/j.neuroimage.2010.03.054

ARTICLE IN PRESS

Benders, M.J., Groenendaal, F., van Bel, F., Ha Vinh, R., Dubois, J., Lazeyras, F., Warfield, S.K., de Vries, L.S., 2009. Brain development of the preterm neonate after neonatal hydrocortisone treatment for chronic lung disease. Pediatr. Res. 66, 555–559.
Buchel, C., Raedler, T., Sommer, M., Sach, M., Weiller, C., Koch, M.A., 2004. White matter asymmetry in the human brain: a diffusion tensor MRI study. Cereb. Cortex 14, 945–951.
Cachia, A., Mangin, J.F., Riviere, D., Kherif, F., Boddaert, N., Andrade, A., Papadopoulos-Orfanos, D., Poline, J.B., Bloch, I., Zilbovicius, M., Sonigo, P., Brunelle, F., Regis, J., 2003. A primal sketch of the cortex mean curvature: a morphogenesis based approach to study the variability of the folding patterns. IEEE Trans. Med. Imaging 22, 754–765.
Chi, J.G., Dooling, E.C., Gilles, F.H., 1977a. Gyral development of the human brain. Ann. Neurol. 1, 86–93.
Chi, J.G., Dooling, E.C., Gilles, F.H., 1977b. Left–right asymmetries of the temporal speech areas of the human fetus. Arch. Neurol. 34, 346–348.
Dehaene-Lambertz, G., Hertz-Pannier, L., Dubois, J., 2006a. Nature and nurture in language acquisition: anatomical and functional brain-imaging studies in infants. Trends Neurosci. 29, 367–373.
Dehaene-Lambertz, G., Hertz-Pannier, L., Dubois, J., Mériaux, S., Roche, A., Sigman, M., Dehaene, S., 2006b. Functional organization of perisylvian activation during presentation of sentences in preverbal infants. Proc. Natl. Acad. Sci. U. S. A. 103, 14240–14245.
Dubois, J., Benders, M., Cachia, A., Lazeyras, F., Ha-Vinh Leuchter, R., Sizonenko, S.V., Borradori-Tolsa, C., Mangin, J.F., Hüppi, P.S., 2008a. Mapping the early cortical folding process in the preterm newborn brain. Cereb. Cortex 18, 1444–1454.
Dubois, J., Benders, M., Borradori-Tolsa, C., Cachia, A., Lazeyras, F., Ha-Vinh Leuchter, R., Sizonenko, S.V., Warfield, S.K., Mangin, J.F., Hüppi, P.S., 2008b. Primary cortical folding in the human newborn: an early marker of later functional development. Brain 131, 2028–2041.
Dubois, J., Hertz-Pannier, L., Mangin, J.F., Cachia, A., Le Bihan, D., Dehaene-Lambertz, G., 2009. Structural asymmetries in the infant language and sensori-motor networks. Cereb. Cortex 19, 414–423.
Feess-Higgins, A., Laroche, J.C., 1987. Development of the human foetal brain: an anatomical atlas. Masson, Inserm-CNRS.
Galaburda, A.M., LeMay, M., Kemper, T.L., Geschwind, N., 1978. Right-left asymmetrics in the brain. Science 199, 852–856.
Garel, C., Chantrel, E., Brisse, H., Elmaleh, M., Luton, D., Oury, J.F., Sebag, G., Hassan, M., 2001. Fetal cerebral cortex: normal gestational landmarks identified using prenatal MR imaging. Am. J. Neuroradiol. 22, 184–189.
Geschwind, N., Levitsky, W., 1968. Human brain: left–right asymmetries in temporal speech region. Science 161, 186–187.
Hüppi, P.S., Schuknecht, B., Boesch, C., Bossi, E., Felblinger, J., Fusch, C., Herschkowitz, N., 1996. Structural and neurobehavioral delay in postnatal brain development of preterm infants. Pediatr. Res. 39, 895–901.
Hüppi, P.S., Warfield, S., Kikinis, R., Barnes, P.D., Zientara, G.P., Jolesz, F.A., Tsuji, M.K., Volpe, J.J., 1998. Quantitative magnetic resonance imaging of brain development in premature and mature newborns. Ann. Neurol. 43, 224–235.
Im, K., Jo, H.J., Mangin, J.F., Evans, A.C., Kim, S.I., Lee, J.M., 2010. Spatial distribution of deep sulcal landmarks and hemispherical asymmetry on the cortical surface. Cereb. Cortex 20, 602–611.
Inder, T.E., Warfield, S.K., Wang, H., Hüppi, P.S., Volpe, J.J., 2005. Abnormal cerebral structure is present at term in premature infants. Pediatrics 115, 286–294.
Jiang, S., Xue, H., Glover, A., Rutherford, M., Rueckert, D., Hajnal, J.V., 2007. MRI of moving subjects using multislice snapshot images with volume reconstruction (SVR): application to fetal, neonatal, and adult brain studies. IEEE Trans. Med. Imaging 26, 967–980.
Kapellou, O., Counsell, S.J., Kennea, N., Dyet, L., Saeed, N., Stark, J., Maalouf, E., Duggan, P., Ajayi-Obe, M., Hajnal, J., Allsop, J.M., Boardman, J., Rutherford, M.A., Cowan, F., Edwards, A.D., 2006. Anormal cortical development after premature birth shown by altered allometric scaling of brain growth. PLoS Med. 3, e265.
Keller, S.S., Crow, T., Foundas, A., Amunts, K., Roberts, N., 2009. Broca's area: nomenclature, anatomy, typology and asymmetry. Brain Lang. 109, 29–48.
Lefèvre, J., Leroy, F., Khan, S., Dubois, J., Hüppi, P.S., Baillet, S., Mangin, J.F., 2009. Identification of growth seeds in the neonate brain through surfacic Helmholtz decomposition. Proceedings of the 21st annual meeting of Information Processing in Medical Imaging (IPMI).
Lyttelton, O.C., Karama, S., Ad-Dab'bagh, Y., Zatorre, R.J., Carbonell, F., Worsley, K., Evans, A.C., 2009. Positional and surface area asymmetry of the human cerebral cortex. Neuroimage 46, 895–903.
Mangin, J.F., Riviere, D., Cachia, A., Duchesnay, E., Cointepas, Y., Papadopoulos-Orfanos, D., Scifo, P., Ochiai, T., Brunelle, F., Regis, J., 2004. A framework to study the cortical folding patterns. Neuroimage 23, S129–S138.
Ono, M., Kubick, S., Abernathey, C., 1990. Atlas of the cerebral sulci. Georg Thiem Verlag.
Regis, J., Mangin, J.F., Ochiai, T., Frouin, V., Riviere, D., Cachia, A., Tamura, M., Samson, Y., 2005. "Sulcal root" generic model: A hypothesis to overcome the variability of the human cortex folding patterns. Neurol. Med. Chir. 45, 1–17.
Rousseau, F., Glenn, O.A., Iordanova, B., Rodriguez-Carranza, C., Vigneron, D.B., Barkovich, J.A., Studholme, C., 2006. Registration-based approach for reconstruction of high-resolution in utero fetal MR brain images. Acad. Radiol. 13, 1072–1081.
Rutherford, M., Jiang, S., Allsop, J., Perkins, L., Srinivasan, L., Hayat, T., Kumar, S., Hajnal, J., 2008. MR imaging methods for assessing fetal brain development. Dev. Neurobiol. 68, 700–711.
Scifo, P., Cachia, A., Boddaert, N., Sonigo, P., Simon, I., Zilbovicius, M., Lethimonnier, F., Le Bihan, D., Brunelle, F., Mangin, J.F., 2003. Antenatal MR imaging for the study of fetus brain development. Meeting of Hum. Brain Mapp. 19, S1589.
Simon, S., Lazeyras, F., Sigrist, A.D., Ecoffey, M., Guatieri, S., Van De Ville, D., Borradori-Tolsa, C., Pelizzone, M., Hüppi, P.S., 2009. Nature vs nurture in newborn voice perception. An fMRI comparison of auditory processing between premature infants at term age and term born neonates. Proceedings of the 17th ISMRM meeting, #3443.
Sowell, E.R., Thompson, P.M., Rex, D., Kornsand, D., Tessner, K.D., Jernigan, T.L., Toga, A.W., 2002. Mapping sulcal pattern asymmetry and local cortical surface gray matter distribution in vivo: maturation in perisylvian cortices. Cereb. Cortex 12, 17–26.
Thompson, D.K., Wood, S.J., Doyle, L.W., Warfield, S.K., Lodygensky, G.A., Anderson, P.J., Egan, G.F., Inder, T.E., 2008. Neonate hippocampal volumes: prematurity, perinatal predictors, and 2-year outcome. Ann. Neurol. 63, 642–651.
Toga, A.W., Thompson, P.M., 2003. Mapping brain asymmetry. Nat. Rev. Neurosci. 4, 37–48.
Tolsa, C.B., Zimine, S., Warfield, S.K., Freschi, M., Sancho Rossignol, A., Lazeyras, F., Hanquinet, S., Pfizenmaier, M., Huppi, P.S., 2004. Early alteration of structural and functional brain development in premature infants born with intrauterine growth restriction. Pediatr. Res. 56, 132–138.
Van Essen DC, 2005. A population-average, landmark- and surface-based (PALS) atlas of human cerebral cortex. Neuroimage 28, 635–662.
Wada, J.A., Clarke, R., Hamm, A., 1975. Cerebral hemispheric asymmetry in humans. Cortical speech zones in 100 adults and 100 infant brains. Arch. Neurol. 32, 239–246.
Warfield, S.K., Kaus, M., Jolesz, F.A., Kikinis, R., 2000. Adaptive, template moderated, spatially varying statistical classification. Med. Image Anal. 4, 43–55.
Watkins, K.E., Paus, T., Lerch, J.P., Zijdenbos, A., Collins, D.L., Neelin, P., Taylor, J., Worsley, K.J., Evans, A.C., 2001. Structural asymmetries in the human brain: a voxel-based statistical analysis of 142 MRI scans. Cereb. Cortex 11, 868–877.
Witelson, S.F., Pallie, W., 1973. Left hemisphere specialization for language in the newborn: neuroanatomical evidence for asymmetry. Brain 96, 641–646.

Please cite this article as: Dubois, J., et al., Structural asymmetries of perisylvian regions in the preterm newborn, NeuroImage (2010), doi:10.1016/j.neuroimage.2010.03.054